

Journal of Materials Chemistry C

Accepted Manuscript



This is an *Accepted Manuscript*, which has been through the Royal Society of Chemistry peer review process and has been accepted for publication.

Accepted Manuscripts are published online shortly after acceptance, before technical editing, formatting and proof reading. Using this free service, authors can make their results available to the community, in citable form, before we publish the edited article. We will replace this *Accepted Manuscript* with the edited and formatted *Advance Article* as soon as it is available.

You can find more information about *Accepted Manuscripts* in the [Information for Authors](#).

Please note that technical editing may introduce minor changes to the text and/or graphics, which may alter content. The journal's standard [Terms & Conditions](#) and the [Ethical guidelines](#) still apply. In no event shall the Royal Society of Chemistry be held responsible for any errors or omissions in this *Accepted Manuscript* or any consequences arising from the use of any information it contains.

ARTICLE

Synthesis, Characterization, and Field-Effect Transistor Performance of Two-Dimensional Starphene Containing Sulfur

Cite this: DOI: 10.1039/x0xx00000x

Received 00th January 2012,
Accepted 00th January 2012

DOI: 10.1039/x0xx00000x

www.rsc.org/Sufen Zou,^{ab} Yingfeng Wang,^a Jianhua Gao,^{*a} Xiaoxia Liu,^a Wanglong Hao,^a Huarong Zhang,^{*a} Haixia Zhang,^{ac} Hui Xie,^a Chengdong Yang,^a Hongxiang Li,^c and Wenping Hu^{*b}

A novel two-dimensional (2D) starphene containing sulfur organic semiconductor material **BTBTT** is synthesized. The spectroscopy, electrochemical and thermostability were investigated and the compound exhibits good stability. The **BTBTT** reveals strong aggregation tendency and forming long single-crystal nanowires evidenced by scanning electron microscopy (SEM) and transmission electron microscopy (TEM). The organic field-effect transistors (OFETs) devices were fabricated based on the thin films and single-crystal nanowires of **BTBTT** respectively, and which exhibit excellent FET performance with a high hole mobility up to $0.56 \text{ cm}^2 \text{V}^{-1} \text{s}^{-1}$ and low threshold voltages.

Introduction

Micro- and nanoscale organic crystals synthesized from π -conjugated molecules have attracted considerable interest as building blocks for organic field-effect transistors (OFETs) due to their single-crystal-like properties.¹ The effective use of small crystals could contribute to integrate these materials into micro- and nano-devices using a “bottom-up” approach which facilitate the device miniaturization.² One-dimensional (1D) nanostructure such as nanowires or nanoribbons is practical advantage in construction of integrated nanoelectronic devices caused by their cofacial molecular stacking along the long-axis of nanowires, since the charge carrier mobility is usually maximized along the direction of cofacial π - π stacking of the molecules.³ However, most 1D nanostructures reported to date are based on inorganic materials, it is a great challenge to develop organic semiconductor materials with controllable aggregation tendency in order to construct micro- and nanoscale organic crystals.

Star-shaped 2D π -conjugated molecules have attracted increasing attention due to their novel structures and potential applications in optical and electrical devices. However, most of the reported star-shaped molecules exhibit low mobility which ranging from 10^{-4} to $10^{-2} \text{ cm}^2 \text{V}^{-1} \text{s}^{-1}$.⁴ The dihedral angle between the core and branched arms which connected by σ -bonds results in a limitation of the effective conjugation.⁵ To eliminate the dihedral angle between the consecutive aromatic rings, a starphene configuration could be valuable alternative

for overcoming the aforementioned drawbacks and affording enhanced π -electron delocalization. The term starphene was coined by Clar and Mullen for benzologues of triphenylene, in which the three branches are annellated to a central ring and radiate outwards in a linear manner.⁶ The completely condensed 2D π -conjugated system of starphene would produce strong intermolecular π - π stacking which is favourable for self-assemble 1D nanostructure.

Herein, we report the synthesis and characterization of a novel 2D starphene containing sulfur benzo[1,2-*b*:3,4-*b'*:5,6-*b''*]tri(benzo[4',5']thieno[2',3'-*d'*]thiophene) (**7**, **BTBTT**). The inserting of thiophene would avoid the deterioration of branched acenes. The spectroscopy, electrochemical and thermostability were investigated and the compound exhibited good stability. The **BTBTT** reveals strong aggregation tendency and forming long single-crystal nanowires evidenced by scanning electron microscopy (SEM) and transmission electron microscopy (TEM). The OFETs devices were fabricated based on the thin films and single-crystal nanowires of **BTBTT** respectively, and which exhibits excellent FET performance with a high hole mobility up to $0.56 \text{ cm}^2 \text{V}^{-1} \text{s}^{-1}$ and low threshold voltages.

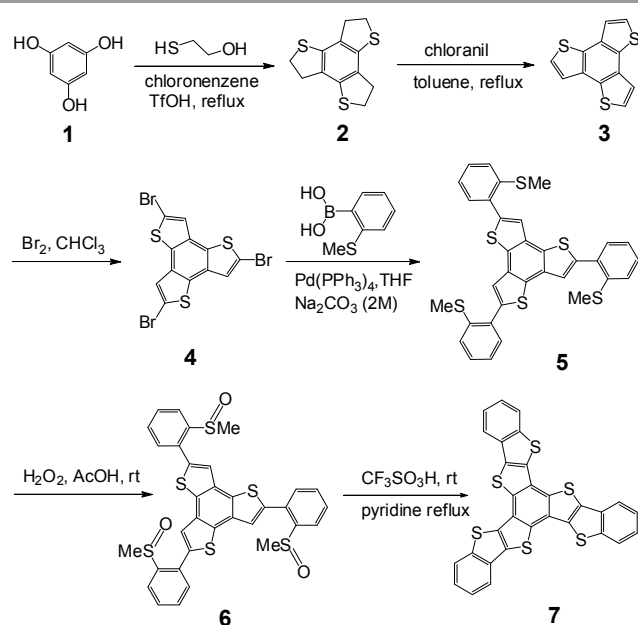
Results and Discussion

Synthesis

The synthesis route of **BTBTT** is presented in Scheme 1 which includes six steps from commercial available 1,3,5-

trihydroxybenzene as starting material. Compounds **2** and **3** were synthesized according to the known literatures.⁷ **3** was brominated and then reacted with 2-(methylthio)phenylboronic acid to give key precursor **5** by the Suzuki coupling reaction with $[\text{Pd}(\text{PPh}_3)_4]$ as a catalyst. The star-shaped precursor **5** was oxidized with 30% aqueous hydrogen peroxide and then intramolecular cyclization with an excess of trifluoromethanesulfonic acid to afford the target product **7**. The intermediate product **6** was used without further purification due to its poor solubility in common organic solvents. The 2D starphene compound **BTBTT** was obtained, and with three benzo[1,2-*b*:4,5-*b'*]dithiophene as the branch arms which fused with the benzene center. The crude product was purified by Soxhlet extraction to give pure **BTBTT** as a pale yellow solid in yield of 45%.

Thermal, optical and electrochemical properties



Scheme 1 Synthesis route of **BTBTT**.

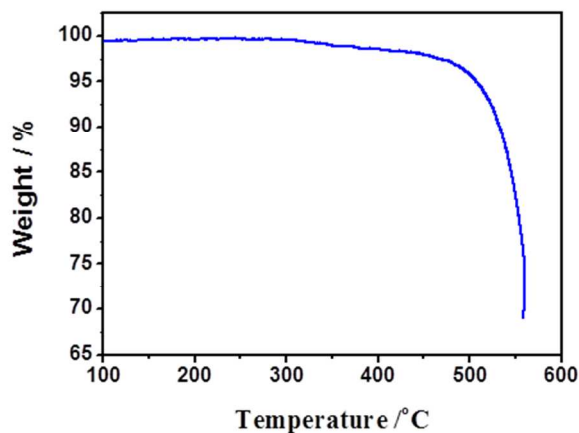


Fig. 1 TGA result of **BTBTT**.

The thermal stability of **BTBTT** was examined by thermal gravimetric analysis (TGA, see Fig. 1). The starphene compound exhibits high thermal stability as indicated by the decomposition temperature (T_d , with 5% weight loss) over 500°C under nitrogen atmosphere.

The UV-vis spectra of **BTBTT** (see Fig. 2) in a dilute dichloromethane solution reveal a strong absorption band at ~280-350 nm and a weaker band at ~450-500 nm. The maximum absorption peak in the solution is located at 484 nm which is corresponding to the π - π^* transition band of the starphene conjugated compound. Compared with the absorption in the solution, the π - π^* transition absorption peak in the thin film vacuum-deposited on quartz is blue-shifted considerable about 120 nm, which indicates that a strong H-aggregate stacking mode was formed due to the strong face-to-face packing (π - π stacking) between the 2D molecules.⁸ The superior aggregation tendency arising from intermolecular π - π interactions is potentially favourable for achieving good OFET performance. The optical energy bandgap of **BTBTT** estimated from the maximal absorption edge in dilute solution was 2.51 eV.

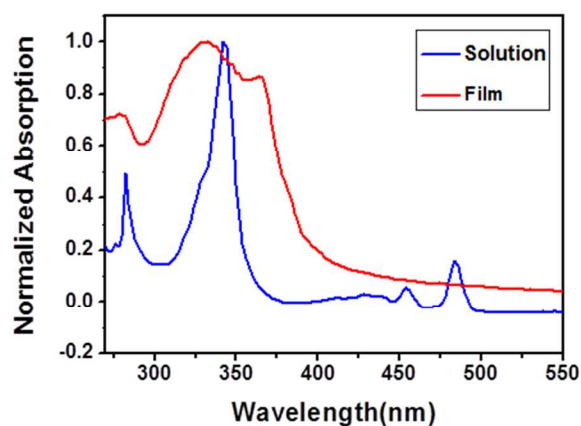


Fig. 2 UV-vis absorption spectra of **BTBTT** dilute solution in CH_2Cl_2 and thin film.

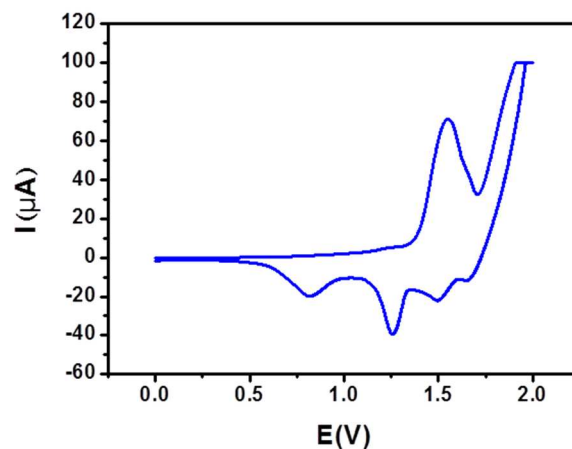


Fig. 3 Cyclic voltammogram of **BTBTT**.

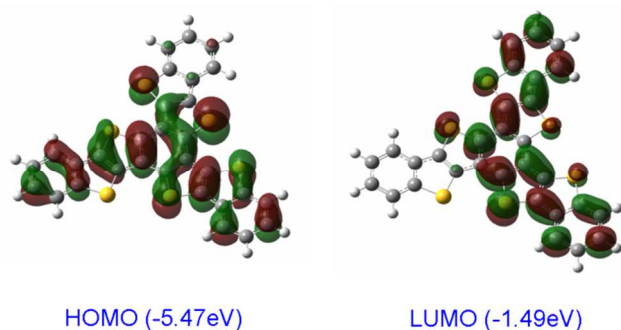


Fig. 4 HOMO and LUMO orbitals of **BTBTT** obtained by using DFT calculations.

The redox properties of **BTBTT** were investigated by cyclic voltammetry (CV) in dichloromethane solution. The indium tin oxide (ITO)-coated glass was used as the working electrode and Ag/AgCl as a reference electrode. The **BTBTT** was deposited onto the ITO electrode by evaporation under vacuum before measured due to its poor solubility. The oxidation peak is 1.55 V and its onset position sites on 1.36 V versus Ag/AgCl (see Fig. 3). The corresponding HOMO energy level was estimated to be -5.76 eV using the equation $E_{\text{HOMO}} = -(4.40 + E_{\text{onset}})$ eV according to literature.⁹ The low-lying HOMO level confirms the high stability of **BTBTT** against oxygen under ambient conditions. Furthermore, the molecular-orbital (MO) calculations of the HOMO and LUMO levels were performed by using density functional theory (DFT) method (B3LYP, 6-31G(d,p)) (see Fig. 4) to clarify the electronic structure of the **BTBTT**. The simulated result reveals that the electron cloud of HOMO and LUMO orbits is not scattered on the whole molecule but dispersed in certain areas, and their distribution directions are different.

Thin films microstructure

The **BTBTT** thin films exhibit a high degree of structural order as evidenced from X-ray diffraction (XRD) measurements (see Fig. 5). Two similar diffraction peaks were observed at $2\theta = 6.2$ and 12.5 degree when deposited on octadecyl-trichlorosilane (OTS) modified SiO_2/Si substrates at different temperature. The d-spacing are estimated to be 1.4 nm and 0.7 nm respectively. This demonstrates that the microcrystalline grains of the thin films have a single preferential orientation which should be dominated by the strong π - π stacking between the 2D molecules.

The surface morphology of **BTBTT** thin films was characterized with atomic force microscopy (AFM) as shown in Fig. 6. AFM images of all the thin films show lamellar structure, the grain size is very tiny when deposited at room temperature. With the increasing of deposition temperature, the surface morphology exhibits distinct terrace-like and the length of grains grows up to micron level. Although the grains connect interactively, the large grains boundary would restrain the migration rate of charge carrier.

1D Singel-crystal nanostructure

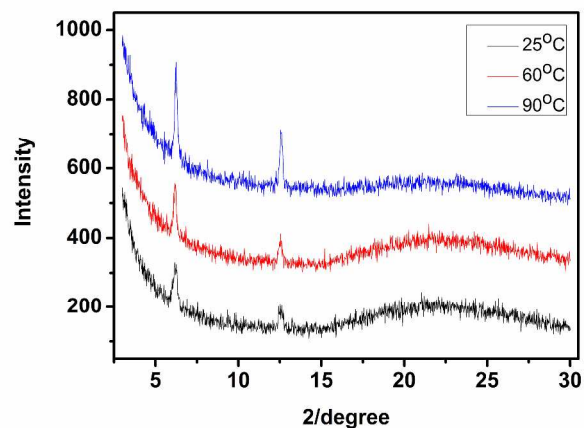


Fig. 5 X-Ray diffraction of **BTBTT** thin films deposited at different substrate temperature.

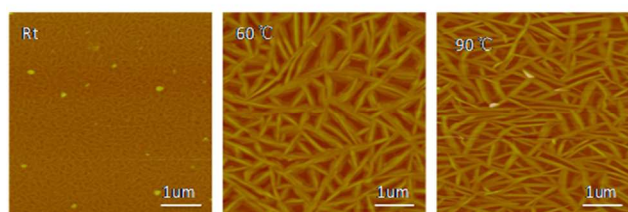


Fig. 6 AFM images of **BTBTT** thin films deposited at different substrate temperature.

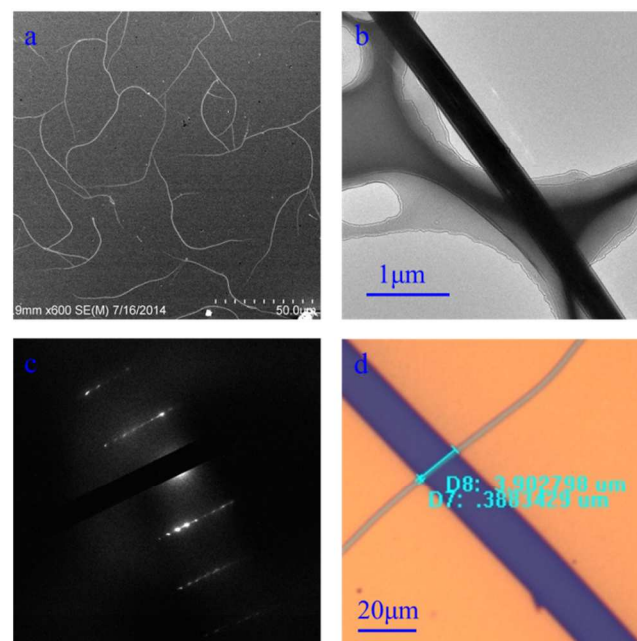


Fig. 7 (a) SEM image of **BTBTT** nanowires, (b) TEM image of **BTBTT** nanowires, and (c) its corresponding electron diffraction pattern, (d) micrograph of FET device based on the **BTBTT** nanowire with the electrode formed by an organic wire mask.

Single-crystal nanowires of **BTBTT** were grown by physical vapor transport method under argon atmosphere at 370°C . Fig.

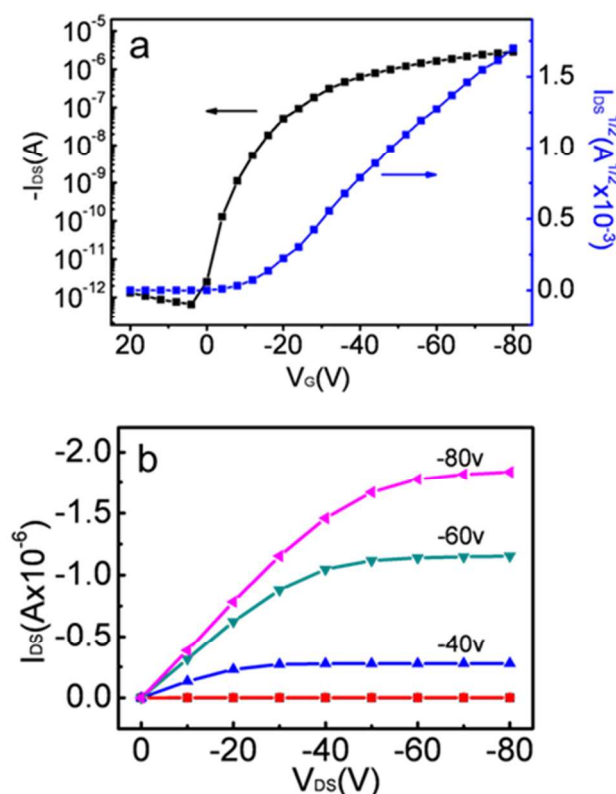


Fig. 8 Transfer (a) and output (b) characteristics for thin film transistor of BTBTT.

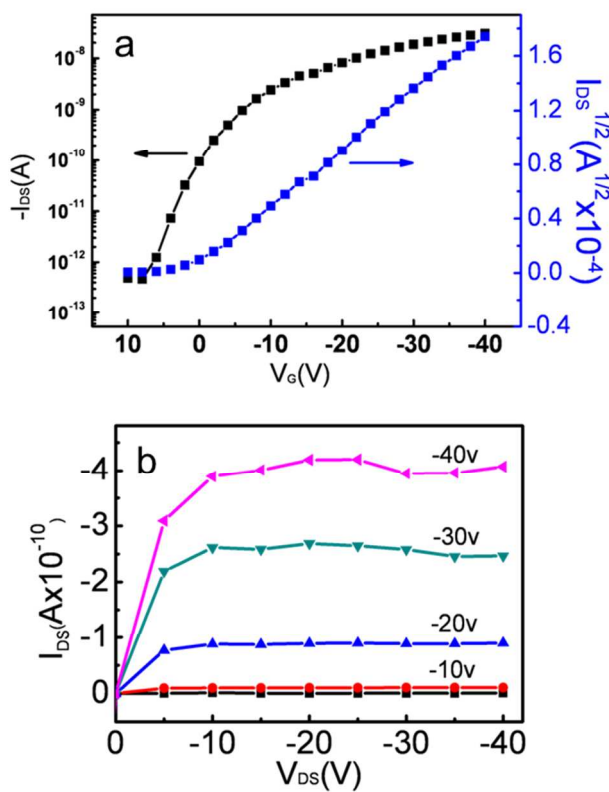


Fig. 9 Transfer (a) and output (b) characteristics for single-crystal transistor of BTBTT.

Table 1 OFET characteristics of BTBTT deposited at different substrate conditions.

$T_{\text{sub}}/^{\circ}\text{C}$	μ (cm^2/Vs)	V_t [V]	On/Off ratio
25	8.17×10^{-3}	-7.04	2.75×10^6
60	2.46×10^{-2}	-20.5	4.87×10^6
90	9.34×10^{-3}	-11.8	2.75×10^6

7a illustrates the SEM image of the nanowires which show 1D molecular assembly with a length up to 100 μm . To further clarify the single-crystal structures nature of the nanowires, the bright field transmission electron microscopy (TEM) and selected-area electron diffraction (SAED) were also executed. The TEM image reveals regular shape of the BTBTT nanowires (Fig. 7b). The corresponding SAED pattern (Fig. 7c) exhibits sharp and well-defined reflection spots, which confirms the single-crystal orientation of the nanowires. Fig. 7d shows the image of FET device based on the individual BTBTT nanowire which observed by optical microscopy (OM).

OFET device performance

To investigate the FET properties of BTBTT, the thin films and single-crystal transistors devices were fabricated based on vacuum-deposited thin films and single-crystal nanowires respectively. The thin film transistors were fabricated with the top-contact configuration and the semiconductor thin films layer were evaporated onto the OTS-modified SiO_2/Si substrates with 50 nm of thickness. Fig. 8 shows an example of typical transfer and output characteristics of BTBTT at $T_{\text{sub}} = 60^{\circ}\text{C}$. All the devices show typical p-channel FET properties under ambient conditions with the mobility calculated from the saturation regime. It was observed that the FET performances for BTBTT depended on the temperature of the substrate, and the FET performance obtained at different deposited temperature is summarized in Table 1. With the increase of substrate temperature, the mobility increased slightly and a high mobility up to $2.46 \times 10^{-2} \text{ cm}^2 \text{V}^{-1} \text{ s}^{-1}$ as well as on/off ratio over 10^6 was obtained at $T_{\text{sub}} = 60^{\circ}\text{C}$. On further increasing the substrate temperature to 90°C , the mobility decreased one order of magnitude. In addition, the thin film devices showed low threshold voltages of $-7.04 \text{ V} \sim -20.5 \text{ V}$.

Single-crystal nanowires of BTBTT were deposited onto the OTS modified SiO_2 substrates. The drain-source (D-S) contacts were fabricated by thermal evaporating a thin layer of Au onto the individual BTBTT single-crystal nanowire and using the "organic ribbon mask technique"¹⁰ at a vacuum pressure of $\sim 10^{-4}$ Pa. The OFET devices were measured in air, and the corresponding transfer and output characteristics were depicted in Fig. 9. The OFET devices based on the BTBTT single-crystal nanowires exhibit high mobility up to $0.56 \text{ cm}^2 \text{V}^{-1} \text{ s}^{-1}$ and on-off ratio of 10^5 . And the average mobility is as high as $0.30 \text{ cm}^2 \text{V}^{-1} \text{ s}^{-1}$ for the fabricated twelve transistors. The high OFET performance should benefit from the strong π - π stack interactions between the 2D π -conjugated molecules.

Experimental section

General

All reagents and chemicals are purchased from commercial sources and used without further purification. Hexahydrobenzo[1,2-*b*:3,4-*b'*:5,6-*b''*]trithiophene (**2**) and benzo[1,2-*b*:3,4-*b'*:5,6-*b''*]trithiophene (**3**) were synthesized according to the known literatures.⁷ ¹H-NMR spectra were recorded on a Bruker DRX-400 spectrometer in deuterated chloroform and DMSO with tetramethylsilane as an internal reference. Mass spectrometry was performed on a TRACE DSQ and MicroTOF-Q II. Elemental analyses were performed by the elemental vario III. The UV-vis spectrum was obtained on a JASCO V-570 UV/vis spectrometer. Thermogravimetric analysis (TGA) was carried out on a PERKIN ELMER TGA7. Cyclic voltammeter (CV) was run on a CHI660C electrochemistry station in a dichloromethane solution using 0.1M tetrabutylammonium hexafluorophosphate (TBAPF₆) as a supporting electrolyte at a scan of 100mV/s, by using ITO as a working electrode, Pt wire as counter electrode. The **BTBTT** was deposited onto the ITO electrode by evaporation under vacuum before measured. AFM images of the film morphology were obtained by a Nanoscope IIIa atomic force microscope in tapping mode. XRD measurements were carried out in the reflection mode using a 2-kW Rigaku X-ray diffraction system.

Thin film transistor device fabrication

FET devices were fabricated by the top contact geometry configuration. The organic semiconductor thin film layer (about 50 nm) was deposited onto OTS treated SiO₂/Si surface. Gold electrodes were deposited by using shadow masks with the channel length and width of 31μm and 273 μm, respectively. The characteristics of the OFET were measured using a Keithley 4200-SCS semiconductor parameter analyzer under ambient conditions.

Single crystal transistor device fabrication

The single-crystal nanowires were grown by physical vapor transport method in a horizontal tube furnace, the **BTBTT** was placed in the ceramic boat at the high-temperature zone of the quartz tube and the OTS treated SiO₂ wafer was at low-temperature. The furnace temperature was increased to 370 °C and then kept at that temperature for 3 h. Finally, the temperature was allowed to descend to room temperature. Then the drain-source (D-S) gold contacts were fabricated on the **BTBTT** single-crystal nanowires by thermal evaporation, using an organic wire as shadow mask.

Synthesis

Synthesis of 2,5,8-Tribromobenzo[1,2-*b*:3,4-*b'*:5,6-*b''*]trithiophene, **4**

To a well-stirred solution of **3** (800 mg, 3.25 mmol) in CH₂Cl₂ (22.7 mL) and acetic acid (5.7 mL) was slowly added N-bromosuccinimide (1.74 g, 9.74 mmol) in small portions. The resulting mixture was stirred at room temperature for 60 h, and

then 10 mL water was added to precipitate the product. The precipitate was collected by filtration, washed with water and ethanol, respectively. After purified by recrystallization from chlorobenzene to give **4** as pale violet needles (1.0 g, 64%). MALID-TOF-MS: m/z 482. ¹H NMR (400MHz, (CD₃)₂SO) δ (ppm): 8.05 (s, 3H)

Synthesis of 2,5,8-Tri(methylthio)benzo[1,2-*b*:3,4-*b'*:5,6-*b''*]trithiophene, **5**

To a solution of **4** (480 mg, 1 mmol) in degassed THF (40 mL) was added 2-(methylthio)phenylboronic acid (510 mg, 3 mmol) and 200 mg Pd(PPh₃)₄. The mixture was stirred under argon for 10 min, and then aqueous NaCO₃ (2 M, 20 mL) was added. The mixture was refluxed for 24 h and cooled to room temperature. After the organic solvent was evaporated, the residue was extracted with CH₂Cl₂, washed with brine and dried with MgSO₄, respectively. The crude product was purified by column chromatography on silica gel with CH₂Cl₂/petroleum (2:3 v/v) as an eluent to yield compound **5** as a pale yellow solid (540 mg, 88%). MALID-TOF-MS: m/z 612; ¹H NMR (400 MHz, CDCl₃) δ (ppm): 7.79 (s, 3H), 7.56 (d, 3H), 7.34-7.40(m, 6H), 7.23 (m, 3H), 2.46 (s, 9H)

Synthesis of benzo[1,2-*b*:3,4-*b'*:5,6-*b''*]tri(benzo[4',5']thieno[2',3'-*d'*]thiophene), **7**, BTBTT

To a solution of **5** (540 mg, 0.88 mmol) in 30 mL glacial acetic acid was slowly added 320 mg H₂O₂ (30%, 2.8 mmol, 3.2 equiv.). The suspension was stirred until dissolved, evaporated in vacuum to give a yellow solid as product **6**. The intermediate product **6** was used without further purification due to its poor solubility in common organic solvents. Then, the product **6** was added to 6mL trifluoromethanesulfonic acid. The resulting solution was stirred for 24 h at room temperature and then slowly poured into a water-pyridine mixture (90mL, 8:1). The yellow precipitate was demethylated by heating to reflux for 12h. The crude product was filtered and washed with CH₂Cl₂ to afford a pale yellow solid. Further purification was carried out by Soxhlet extraction (223 mg, 45%). MALID -TOF-MS: m/z 564. Anal.calcd for C₃₀H₁₂S₆: C, 63.80; H, 2.14; S 34.06. Found: C, 63.67; H, 2.24; S, 32.84.

Conclusions

In summary, a novel 2D starphene derivative **BTBTT** is synthesized. This material possesses high stability which was confirmed by TGA, UV-vis spectra and cyclic voltammetry. The crystallinity and morphology of the semiconductor thin films were characterized by XRD and AFM respectively. A mobility up to 2.46×10⁻² cm²V⁻¹s⁻¹ and on-off ratio larger than 10⁶ could be achieved for the thin film transistor. The single-crystal transistor devices based on the **BTBTT** nanowires exhibit high mobility up to 0.56 cm²V⁻¹s⁻¹ and on-off ratio of 10⁵. The high mobility demonstrated that it is useful for forming strong aggregation thus enhancing charge carrier transport by elimination of the dihedral angle. The single-crystal structures nature of the nanowires was confirmed by the bright field TEM and corresponding SAED pattern. The greater

single crystal is growing and better single-crystal OFET device performance could be anticipated.

Acknowledgements

The present research was financially supported by the National Natural Science Foundation of China (51003022, 21272049), the Ministry of Science and Technology of China (2013CB933500). Sufen Zou and Yingfeng Wang contributed equally to this work.

Notes and references

^a Key Laboratory of Organosilicon Chemistry and Material Technology of Ministry of Education, Hangzhou Normal University, Hangzhou 311121, P. R. China. Fax: +86-571-28865135; Tel: +86-571-28865135; E-mail: gaojh@hznu.edu.cn.

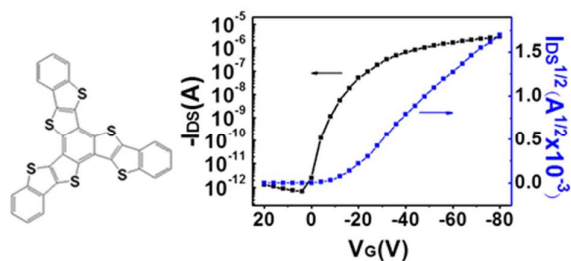
^b Key Laboratory of Organic Solids, Institute of Chemistry, Chinese Academy of Sciences, Beijing 100190, P. R. China. Tel: +86-10-82615030; E-mail: huwp@iccas.ac.cn.

^c Laboratory of Materials Science, Shanghai Institute of Organic Chemistry, Chinese Academy of Sciences, Shanghai 200032, P. R. China. Tel: +86-21-54925024; E-mail: lhx@mail.sioc.ac.cn

- C. Reese, W. Chung, M. Ling, M. Roberts and Z. Bao, *Appl. Phys. Lett.*, 2006, **89**, 202108; Q. Tang, H. Li, Y. Liu and W. Hu, *J. Am. Chem. Soc.*, 2006, **128**, 14634; A. L. Briseno, M. Roberts, M.-M. Ling, H. Moon, E. J. Nemanick and Z. Bao, *J. Am. Chem. Soc.*, 2006, **128**, 3880; Q. Tang, H. Li, Y. Song, W. Xu, W. Hu, L. Jiang, Y. Liu, X. Wang and D. Zhu, *Adv. Mater.*, 2006, **18**, 3010; S. Xiao, J. Tang, T. Beetz, X. Guo, N. Tremblay, T. Siegrist, Y. Zhu, M. Steigerwald and C. Nuckolls, *J. Am. Chem. Soc.*, 2006, **128**, 10700; Q. Tang, H. Li, M. He, W. Hu, C. Liu, K. Chen, C. Wang, Y. Liu and D. Zhu, *Adv. Mater.*, 2006, **18**, 65; A. L. Briseno, S. C. B. Mannsfeld, X. Lu, Y. Xiong, S. A. Jenekhe, Z. Bao and Y. Xia, *Nano Lett.*, 2007, **7**, 668; D. H. Kim, D. Y. Lee, H. S. Lee, W. H. Lee, Y. H. Kim, J. I. Han and K. Cho, *Adv. Mater.*, 2007, **19**, 678; L. Jiang, W. Hu, Z. Wei, W. Xu and H. Meng, *Adv. Mater.*, 2009, **21**, 3649; R. Li, L. Jiang, Q. Meng, J. Gao, H. Li, Q. Tang, M. He, W. Hu, Y. Liu, and D. Zhu, *Adv. Mater.* 2009, **21**, 4492; X. Liu, Y. Wang, J. Gao, L. Jiang, X. Qi, W. Hao, S. Zou, H. Zhang and W. Hu, *Chem. Commun.*, 2014, **50**, 442.
- R. Li, W. Hu, Y. Liu and D. Zhu, *Acc. Chem. Res.*, 2010, **43**, 529.
- L. Zang, Y. Che and J. S. Moore, *Acc. Chem. Res.*, 2008, **41**, 1596; Y. Che, A. Datar, X. Yang, T. Naddo, J. Zhao and L. Zang, *J. Am. Chem. Soc.*, 2007, **129**, 6354; Y. Che, A. Datar, K. Balakrishnan, L. Zang, *J. Am. Chem. Soc.*, 2007, **129**, 7234.
- A. L. Kanibolotsky, I. F. Perepichkaz and P. J. Skabara, *Chem. Soc. Rev.*, 2010, **39**, 2695; T. Jarosz, M. Lapkowski and P. Ledwon, *Macromol. Rapid Commun.*, 2014, **35**, 1006; J. Roncali, P. Leriche and A. Cravino, *Adv. Mater.*, 2007, **19**, 2045.
- Y. Nicolas, P. Blanchard, E. Levillain, M. Allain, N. Mercier and J. Roncali, *Org. Lett.*, 2004, **6**, 273.
- E. Clar and A. Mullen, *Tetrahedron*, 1968, **24**, 6719.
- B. Rungtaweivoranit, A. Butsuri, K. Wongma, K. Sadorn, K. Neranon, C. Nerungsi and T. Thongpanchang, *Tetrahedron Lett.*, 2012, **53**, 1816.
- S. Hotta, Y. Ichino, Y. Yoshida and M. Yoshida, *J. Phys. Chem. B*, 2000, **104**, 10316; M. S. Kim, E. H. Cho, D. H. Park, H. Jung, J. Bang and J. Joo, *Nanoscale Res. Lett.*, 2011, **6**, 405; E. G. Mdrae, M. Kasha, Physical processes in radiation biology, A. G. Augenstein, R. Mason, R. Rosenberg (Eds), New York: Academic Press, 1964.
- Y. Zhou, L. Wang, J. Wang, J. Pei and Yong Cao, *Adv. Mater.*, 2008, **20**, 3745; W. Y. Wong, L. Liu, D. Cui, L. M. Leung, C. F. Kwong, T.-H. Lee and H.-F. Ng, *Macromolecules*, 2005, **38**, 4970.
- L. Jiang, J. Gao, E. Wang, H. Li, Z. Wang, W. Hu and L. Jiang, *Adv. Mater.*, 2008, **20**, 2735.

Table of Contents

Colour graphic:



Text:

A novel starphene containing sulfur exhibits excellent FET performance with a mobility of $0.56 \text{ cm}^2\text{V}^{-1}\text{s}^{-1}$ based on the single-crystal nanowires.